INTRODUCTION

Studies of the structure of the crystal structures, the nature of phase transitions recently reached a qualitatively new level. By theoretical and experimental work has been formulated a universal approach to the description of phase state on the basis of solving discrete field theory models. In the language of the theory of interacting nodes on harmonic lattice spins have been found and studied nonlinear solutions in the form of fermions. At the same time, as it turned out, the system can be represented by the normal fermion modes. The theory of the soft mode condensation Goldstounovskogo boson is just a special case of solutions in the form of single-particle fermion states - for example, the spin-wave or soliton.

Theoretical and experimental studies carried out for the external magnetic field and take into account only the spin-spin interaction in the framework of models with different dimensionality, showed that the behavior of the system depends not only on the spin and spatial dimension of the system, but. must be considered a significant radius interspin interaction. It has been found that in this case there are classes of solutions to form the long-period structure, and observed experimentally.

In recent years, were discovered and studied compounds with charge density waves, quasi-one organic semiconductors and dielectrics, in which it was found ordering various elements of the structure similar to the long-period form of magnets.

Unlike magnetic systems in dielectric crystals at the forefront of the dipole-dipole interaction and the dimension of the spin variable gives way pseudospin ordering chemical bonds. In crystalline dielectrics with a structure of β-K_2SO_4 were first detected with an incommensurate phase, compared with the original sample intervals. From X-ray data indicated that the emerging superstructure reflections can be characterized by a temperature dependent parameter disparity.

Change the local environment of the structural units in phases with such features more optimal way to observe change of the electric field, or its constituents. Therefore, the method of nuclear quadrupole resonance (NQR) observed in the nucleus with the quadrupole moment and depends on the electric field gradient at the nucleus under study, is optimal for the study of incommensurate structures. Nucleus Cl, Br, J in crystals of the family A_2BX_4 occupy a convenient structural position and allow to obtain information about the origin of the primary structural disproportion, the type of phase transition, modulation features.

With the participation of the author have been made one of the first such studies, including those under the influence of high hydrostatic pressure. Involvement of the latter, as an additional parameter allows you to get a new non-trivial information about the incommensurate phase.

The objectives of this thesis include studies by nuclear quadrupole resonance of halogens (Cl, Br, J), and other methods, crystals family β-K_2SO_4 with structural disproportion. Elucidation of changes in the spectral features of the resonance parameters in phase transitions and symmetry transformations, the analysis of the local environment and the nucleus of its transformation into different compounds of this series with temperature and high hydrostatic pressure. Investigation of the processes of the spin dynamics. In combination with other methods of analysis of changes in the crystal symmetry at structural phase transitions.

Chapter 1. Disproportionately modulated phases in dielectrics with structure type β-K_2SO_4.

§ 1.1.Theory of phase transitions and incommensurate phases.

Phase transition is called structural when changes-crystallographic structure of matter. Symmetry of the crystal lattice, as it is known, in the general case described simorfnymi 230 space groups. Change in the symmetry of the crystal at the phase transition seemed, until recently, in the framework of the Landau-Devonshire, as a change of some function, called the order parameter, by the loss of the symmetry elements and decreasing the initial symmetry G_o to a certain subgroup of the symmetry group G_1 G_o.

From the point of view of the atomic structure of the crystal, this means that the asymmetric atoms in the G_1 phase, shifted relative to the equilibrium positions which they occupy at the high phase. The structure of the new phase G_1 is a superposition of the displacements corresponding frozen soft mode and structure of G_0 phase. Hence the structure of the new phase is uniquely determined by the structure of the initial phase and the vector of the soft mode (the symmetry of the soft mode).

According to Anderson's theory [1], phase transitions caused by the instability of the crystal relative to some of its normal modes in the high-temperature phase. The frequency of this mode decreases when approaching the critical temperature T_i, and the restoring force for displacements corresponding to such a fashion tends to zero as long as the phonon does not condense on the stability boundary. Consequently, the static displacements of atoms at the transition from phase G_0 to G_1 phase are frozen vibrational displacement codes corresponding to the soft phonon (q_s).

However, this concept is applicable when the displacements of atoms from the high-small positions (phase transitions of bias) and becomes less useful for large displacements (phase transitions of the order-disorder).

In the latter case, structural changes are usually described in the framework of the Ising model, which deals with large-scale motions and entered the (pseudo) spin variables describing the position of atoms or groups. The results of this approach generally boil down to the fact that the phase transition occurs at the wave vector q_s, which corresponds to a maximum of interactions J(q) between objects Ising nodes.

Parallel - the development of theory undertaken considerable experimental efforts to study the microscopic nature structure phase transitions. Most known results of the classical study of the temperature dependences of q_s in β-K_2SO_4 [2]. Neytron - diffraction method on this crystal were shot dispersion curves q(ω) at different temperatures Figure 1.1. Temperature dependence of q for S_2 fashion shows that the wave rector q_s can have values between zero and the wave vector at the Brillouin zone boundary. In this case, the value , corresponding to a minimum the dispersion curve, the symmetry is not fixed and typically depends on the temperature.

Changes in the structure of the crystal in this case determined by the symmetry of high-G_0 phase, followed by some pretransitional area corresponding mitigation fashion responsible for the phase transition at T_i. Below T_i there is a phase where the minimum of the soft mode varies near the symmetrical point of reciprocal space G*, and when they correspond exactly q_s G*, at T_c transition occurs in the low-symmetry structure. The phase

between T_i and T_c is called, incommensurat because values of the wave vector $q_{s,}$ when it is a continuous change can take irrational values, which corresponds to an infinitely large unit cell of the crystal. In this case the crystal is represented three-dimensionally periodic structure, where any inside – crystalline function in one or more directions superimposed long-wavelength spatial modulation period is generally not a multiple of the period of the unit cell of high-symmetry phase. Displacement of nucleus of symmetric function of the order parameter in this

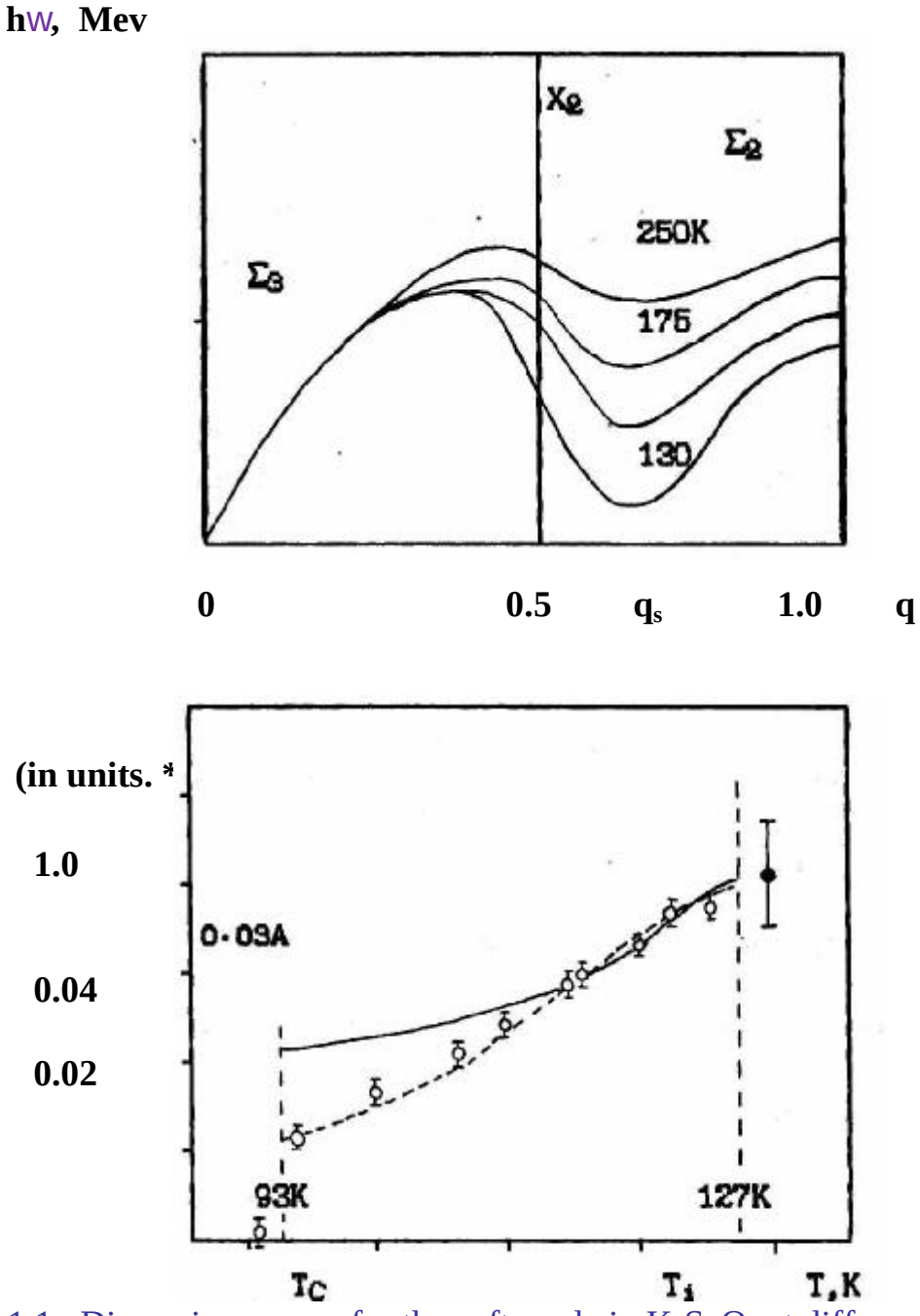

Figure 1.1. Dispersion curves for the soft mode in K_2SeO_4 at different temperatures and the dependence $q_S=1/3(1-\delta)\times 2\pi/a$.

case, can be represented by an expansion in the eigenvectors of the soft mode [2,3]:

$$u_{lkp}=\{\sum_{\lambda} A`_{\lambda} \times \vec{e}_k^{\,l}+\sum_{\lambda} A_{\lambda} \times[\vec{e}\times\vec{X}(lk)]\} \times \exp 2\pi i(qx_l + \varphi).. \quad (1.1.)$$

where e_k^l - eigen vectors irreducible representation G*; $A`_{\lambda}$, A_{λ} - amplitude eigenvectors; X (lk) – l-st position of the atom, the center of mass of k-th group in the p-th unit cell; j -wave phase modulation.

Analysis of the interaction of atoms in an external periodic potential shown [4,5] that the period of the structure is fixed on the true meaning and proportioned incommensurate phase is not realized. The resulting wave vector, depending on the "pressure", varies continuously, but Nonanalytic. For this strange behavior, mathematicians devised a very original name - "Devil's Staircase" (devil or Satan staircase) [5]. However, initially there was no hope to explore different types of non-analytic behavior numerically, and even more so by experiment.

In addition to the theory of Aubrey [5,6], in [7,8,9], to describe the transition from incommensurate (Jc) to the commensurate phase were introduced "domain" wall or soliton theory and developed the idea as part of Macmillan Ising models with solitons, phasons and "devil's staircase".

Results McMillan, reduced to the fact that the transition from J_C in the commensurate phase can be represented by a picture of soliton-like structure of the atomic displacements described by the soliton (domain) wall :

$$\mathbf{u = A \cos j\,(x);\ j\,(x) - k/p\ arctg(exp(-ax/p))} \quad (1.2)$$

j **(x)**2p/p; p = 1,2,...k. These walls separate regions with different values of the phase shifts of atoms j **(x)** = 2p/p; p = 1,2,...k.. Shape of the phase function in the incommensurate (incommensurate) phase is given by:

$$\mathbf{j\,(x)} = j_o + \frac{2\pi m}{p} j\,(x\text{-}mb) \quad (1.3)$$

where j_o - the phase shift; distance between the walls, m = 1,2,3, ... p.

When the temperature decreases, the width of the soliton wall and a^{-1} is a continuous transition to the commensurate state. Order parameter in this case is the number of solitons.

In real crystals, if the width of the soliton is a few lattice periods, the center of the soliton is energetically advantageous to have at some point in the unit cell [10]. In this case, the transition to the final as symmetrical, the system will experience a sequence of phase transitions of the first kind, until you reach the main phase with p = k. In addition, there are often a few stars of the wave vectors that lead to the existence of incommensurate walls of various types, and can be carried out transitions between different configurations of the soliton structure.

There are other types of non-linear numerical solutions (kinks, wobblers, etc.), describing the shape of the atomic displacements in the incommensurate phase. Such as

$NaNO_2$, the structure seems almost plane waves, and up to T_C no harmonics incommensurate wave vector [11].

McMillan ideas were developed Janson[8] Aubrey [12]and Buck [13] These authors studied the behavior of soliton solutions of the discrete problem in Ising-like systems with the interaction up to three neighbors (ANNNI - model). In this case, the deviation of the wave vector q_d = (1-)*/3 proportioned values can be represented by a rational number x = M/N, and the structure of solutions (steps "devil's staircase") may be associated with symmetry interconnected sublattices with symmetry restrictions on the values of the numbers N and M. Then the transition from the high-G_0 in the low-symmetry phase G_i, between the phase diagram there is a region where the structure is represented by a cascade of intermediate or long-period incommensurate states with discrete or continuous variation of the wave vector q_d (Fig.4.38 and 4.39). The regions of these states are very sensitive to external (theoretical) effects.

By this time the state of the theory of symmetry was enough to make its results for the classification of all possible types of theoretical incommensurate structures [15] and classify them into different classes incommensurate space groups in the theory of supersymmetry [16].

Supersymmetry transformation rules allow you to specify the direction of the transformation and permissible types of symmetry of incommensurate structures that can realistically be implemented in each class Fedorovskoye crystal structure.

As an illustration, we give an outline of possible directions changes in lattice symmetry Brillouin highly symmetric group D_{2h}^{16} (Pnma), Figure 1.2. In the circles of indexed figures experimentally realized soft modes for crystals 1) $Tb_2(Mo0_4)_3$, k_m = p (110) 2) $RbD_3(Se0_3)_2$, k_z = p (001) 3) K_2SeO_4 , k = 2p (m00) m»1/3 In [18] is a diagram indicating the possible ways of symmetry transformations structure Pnma (D_{2h}^{16}).

From the experimental data revealed that the sequence of phase transitions in crystals with high-symmetry group symmetry Pnma structure β-K_2SO_4 defines mitigation dispersion curve along the S line. There are four irreducible representations of S_1, S_2, S_3, S_4 of this group. In K_2SeO_4, for example, the soft mode associated with the representation of S_2:

E-line E-line

D_{2h}^{16} (Pnma) ---------® Jc modulation --------® C_{2v}^{9} ($Pna2_1$)

m»1/3 along the x-axis m»1/3

Later in other compounds of the family A_2BX_4 type structure β-K_2SO_4, installed other possible sequences of symmetry transformations, which are determined by another basis of irreducible representations of D_{2h}^{16} (Table 1.1).

Given the possibility of experimental observation of the behavior of "devil's staircase" or to account for the influence of concomitant and secondary order parameters, the analysis of experimental structural data necessary to know the various ways allowed symmetry transformations of the structure, taking into account the parity ratio x= N/M in the case of long-period structures . The analysis performed in Refs [17, 18], which indicates all possible subgroups generated representations S_i, L_i, G_i

The above theory of solids based on the adiabatic or Born-Oppenheimer approximation, where the kinetic energy of the nucleus T ($R_{n)}$ is actually neglected. However, as the last experimental studies [23], the characteristic times of nuclear motions can be compared with the electronic. Arise in this case, the vibronic interaction, even in the case of mixed singlet states, lead to Jahn-Teller distortions, which crystal system can be a source of instability and dipole explain the nature of ferroelectricity [22]. From the standpoint of the vibronic theory postulates soft mode are consequences of the cooperative pseudo-Jahn-Teller effect. In the framework of this theory can be explained and the disproportionate nature of the state in dielectric crystals. Interaction of the electron or nuclear state leads to interaction pseudo-soft phonon modes of different symmetry, localized near a variety of provisions of the reciprocal lattice symmetry [8, 94]. In the high-temperature phase $G_{0,}$ these modes do not interact, but below the temperature will determine the resonant interaction of the two components of the structure, phase-shifted. From

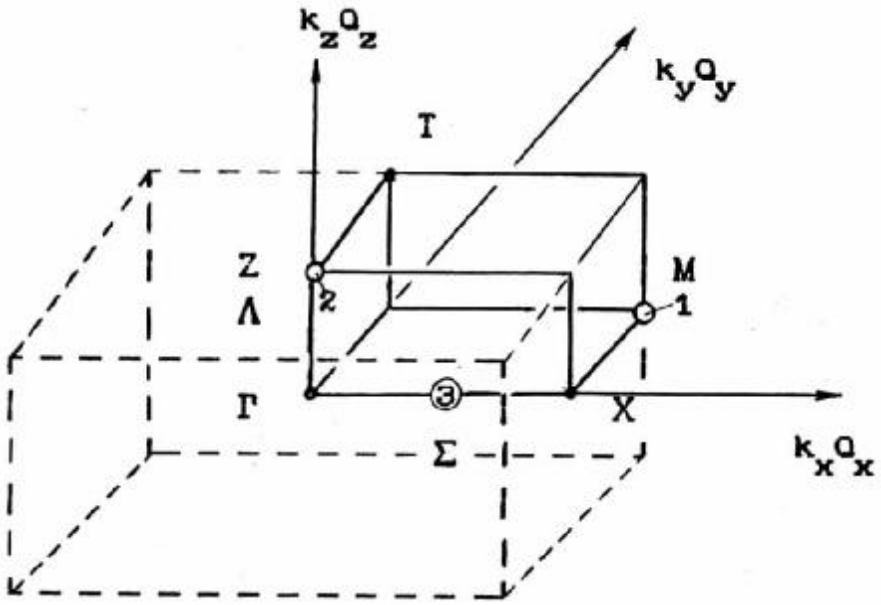

Figure 1.2. Symmetric points and directions of the lattice Brillouin grupy D_{2h}^{16} (Pnma).

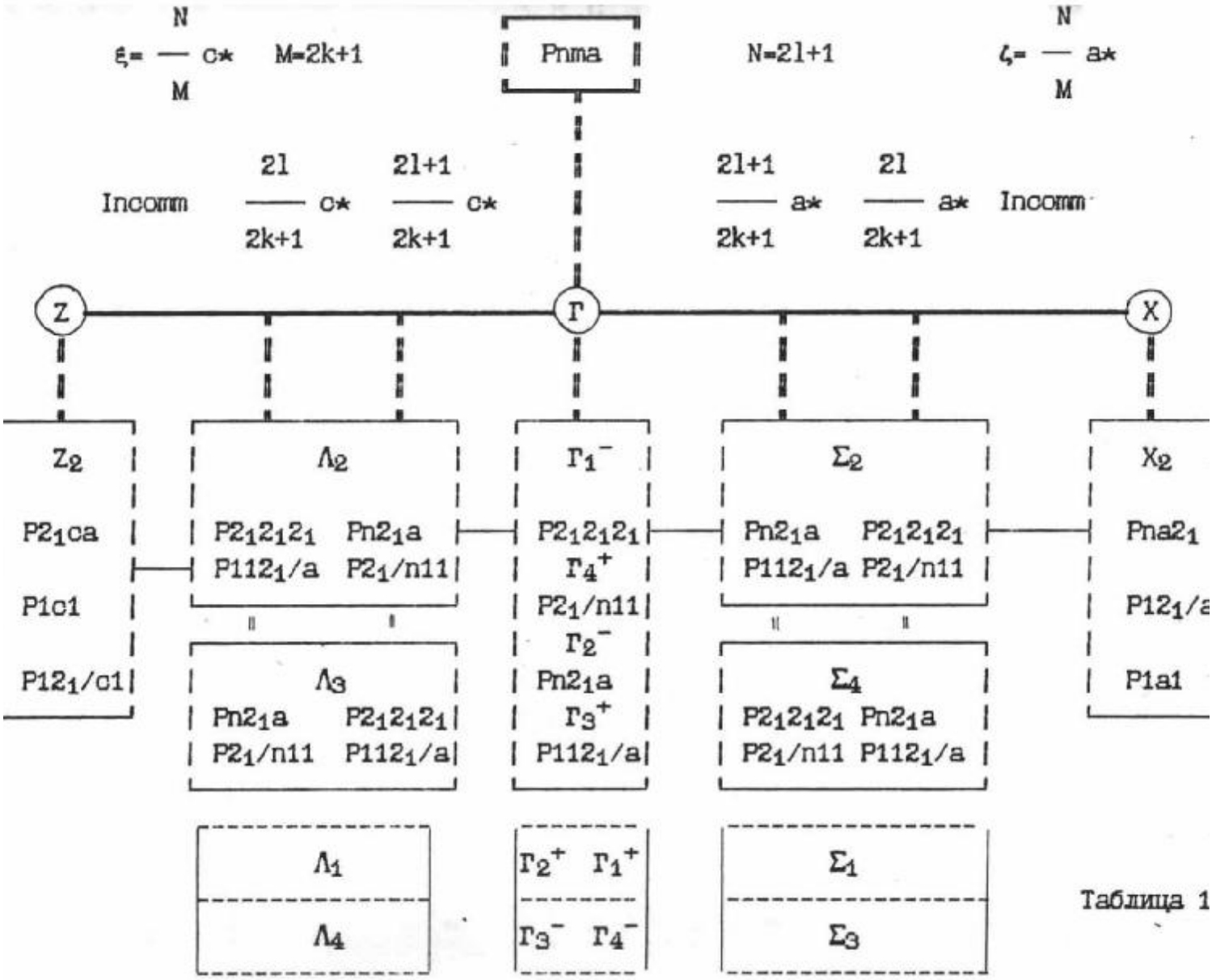
ξ= N/M c* M=2k+1
Pnma
N=2l+1 ζ= N/M a*
Incomm 2l/2k+1 c* 2l+1/2k+1 c*
2l+1/2k+1 a* 2l/2k+1 a* Incomm
Z
Γ
X
Z2
P2₁ca
P1c1
P12₁/c1
Λ2
P2₁2₁2₁ Pn2₁a
P112₁/a P2₁/n11
Λ3
Pn2₁a P2₁2₁2₁
P2₁/n11 P112₁/a
Γ1⁻
P2₁2₁2₁
Γ4⁺
P2₁/n11
Γ2⁻
Pn2₁a
Γ3⁺
P112₁/a
Σ2
Pn2₁a P2₁2₁2₁
P112₁/a P2₁/n11
Σ4
P2₁2₁2₁ Pn2₁a
P2₁/n11 P112₁/a
X2
Pna2₁
P12₁/a
P1a1
Λ1
Λ4
Γ2⁺ Γ1⁺
Γ3⁻ Γ4⁻
Σ1
Σ3

Таблица 1

the standpoint of the atomic arrangement of this will lead to cooperation between the two sublattices of the crystal with different periods and realized a disproportionate or mosaic-cluster state.

Recently, efforts have been made to combine the universality hypothesis and cluster theory of phase transitions. In this way on the basis of experimental data for the theoretical foundations of association phase transitions of receiving and order-disorder [19,20]. There are reasonable grounds to believe that these transitions differ only in magnitude of the contribution from the phonon modes and pseudospin. This theory considers the equilibrium configurations of atoms in direct space:

$$H=\sum_l \left\{ \frac{1}{2}u^2(l) + V_S\left\langle u(l)\right\rangle \right\} + \frac{c}{2}\sum_l [u(l) - u(l')]^2 \quad (1.4)$$

with single-particle potential:

$$V_s(u) = \frac{A}{2}u^2 + \frac{B}{4}u^4 + \ldots$$

In contrast to the models discussed above is introduced varying degrees of anharmonicity motion near double-well potential. In the case where the value of $g = V°_s/K_S T_C$ (ratio of the depth of the pit to the local thermal energy) is small, the offset describes weakly damped mode, otherwise the soft mode is strongly overdamped, and there is strong anharmonicity of the atomic motion in the potential V_s (g>l). In the latter case, at low temperatures (below $T_{C)}$ one of the holes has a large population. As numerical calculations before T_C there Pretransitional area where there are buds (clusters), whose structure is similar to the structure of the low-temperature phase. Finite lifetime and size correlated moving clusters form different from that of the matrix, a dynamic structure, which is manifested in the spectral response function of the system. Molecular dynamics method were obtained solving the equations of motion with the Hamiltonian (4) as a nonlinear soliton solutions. In case of submission of solitons in the form of pseudo-ideal gas particles, the spectral function of the system is described as a phonon spectrum plus scattering due to slower movement of clusters (Gallo, diffuse bands on radiographs). When the speed of the cluster (or its borders) greater than the change in its size, there is a critical narrowing of the spectral components (central peak). Or, in the case of bias, if the fluctuations around quasi offset provisions are large compared with the quasi-equilibrium by the local displacements.

Even for small fluctuations in the presence of correlated moving regions should lead to redistribution contribution to the spectral response function between the quasi-harmonic frequencies and part responsible for the cluster scale movement.

Thus, even if the bias (g « 1), the spectral function of the coordinate ordering Q completely changed at $T_i > T_C$ with decreasing T. For $T < T_i$ soft phonon spectrum into the growth of the central peak. In systems offset soft mode has a resonant nature, although it may be a bit muted (Re and Im parts different from zero). In systems of order-disorder imaginary part of the soft mode is always different from zero, a Re part only if the quantum mechanical ground state splitting (tunneling, H-bonds). Cluster pattern in the transition of the displacement type allows crossover from mode to mode bias order-disorder at $T > T_{c,}$ as a result of the coherence of atomic motions.

Temporal and spatial correlation functions of clusters, also have considerable scale range. Maximum size and lifetime limited correlation length and time, and the minimum value - the size of embryos and their lifetime indevelopment threshold temperature fluctuations. If the system causes an increase in the size of preventing germs time structural redistribution could increase significantly and experimentally observed complete or partial freezing of non-equilibrium state of the system (windows). In the thermodynamic sense, the surface free energy of the system in the microscopic space of external parameters is represented by many local minimums separated by high energy barriers which may exist for a long time long-lived metastable *phases* overlapped with the topological structure (quasi-ergodic behavior) [21].

The problem of implementation of some elements of the crystal structure in a state such as glass, under quasiergodic assumptions led to the development of new approaches in the thermodynamic description of phase transitions. Quasiergodic system under certain conditions can evolve different structural time-dependent pathways in megascopic (cluster) and the macroscopic sense. In this case also, there is certain temperature $T_к$, the separating region with various types of thermodynamic behavior.

§ 1.2 Radiospec research methods disproportionately modulated structures.

Radiospectroscopic research methods substances based on excitation of transitions between energy levels of nuclear spins by the RF field. In the case of crystalline solids RF interaction with nuclear or electron spins in a crystal field representation atoms in the form of:

$$H = H_0 + H_1 + ... \qquad (1.6)$$

where **Ho** is **about** - the interaction Hamiltonian of the spin of an electron-nuclear environment of crystal atoms, $\mathbf{H_1}$ - interaction of the RF field.

In general terms, in connection with the usual symmetry of the nuclear wave functions, crystal-field Hamiltonian **H** atoms can be represented by a series expansion in even powers of the spin moments [19,24]:

$$(1.7) \quad H_0 = \sum_{-2}^{2} V_2^m Q_2^m + \sum_{-2}^{2} V_4^m Q_4^m + ...$$

where Q_i - operators associated with the projection of the spin operators; $V_i^{m,}$ - coefficients, expressed in terms of parameters inside and interatomic interactions. Symmetry of these factors, in particular, depends on the symmetry of the crystal lattice and the phase transition is mainly determined by the symmetry of the soft mode.

In the case of nuclear quadrupole resonance (NQR) the interaction of spherically asymmetric nucleus of an atom with an inhomogeneous electric field electron environment. Coulomb energy of this interaction is given by [25]:

$$H_0 = \int\int \frac{\rho_e \rho_n dV_e dV_n}{|r_n - r_e|} \qquad (1.8)$$

where ρ_e and ρ_n - density of electron and nuclear weapons; $\mathbf{r_n}$-$\mathbf{r_e}$ - distance between the interacting charge volume $\mathbf{dV_e}$ $\mathbf{dV_n}$. Using the decomposition

$$\frac{1}{|r_n - r_e|} \sum_{l=0} \sum_{m=-1} \frac{4\pi r_n^l}{(2l+1) r^{l+1}} Y_l^m(\theta_n, \varphi_n) Y_l^{-m}(\theta_l, \varphi_l) \qquad (1.9)$$

in spherical and radial functions and introducing the notation V_i for the l-th term in the expansion potential of the dipole moments of the electron nucleus

$$V_l^m = \sqrt{4\pi/(2l+1)} \int \frac{\rho_e}{r_l^{l+1}} Y_l^m(\theta_e \varphi_e) dv_e \qquad (1.10)$$

$$Q_l^m = \sqrt{4\pi/(4l+1)} \int \rho_n r_n \frac{\rho_e}{r_l^{l+1}} Y(\theta_n \varphi_n) dv_n$$

and passing to the operators, we obtain the interaction Hamiltonian nuclear electric moment with the atomic electrons in the form (1.7). Nuclear quadrupole interaction is described by the term

$$H_Q = \sum_{-2}^{2} V_2^m Q_2^m \qquad (1.11)$$

where, as is well known [24], the operators Q_2^m expressed in terms of the operators of the nuclear spin I, I_z, I_-, I_+, and the components of V_2^m through komponty EFG tensor q_{ab}:

$$v_2^{-m} = \sum_{a,b=x,y,z} a_2^{-m} q_{ab} d_{ab}^{-m}; \quad \text{, где} \quad q_{ab} = \frac{d^2}{dX_a dX_b} \int \frac{\rho_{ei}}{r_i} dv_e \qquad (1.12)$$

In the simplest approximation is considered point-charge model, oscillating near the sites of the crystal lattice r_i.

$$q_{ab} = \sum \frac{\partial^2}{\partial X_a \partial X_b} \frac{e_i}{r_i} = -\sum_{ab} \frac{e_i (3X_a X_b - d_{ab} r_i^2)}{r_i^5} \qquad (1.13)$$

Returned to the expression (1.7), we see that the coefficients of V_2^m,4 are determined, in particular the nature of the atomic displacements in the crystal and in the general case can be presented through static and dynamic displacements of these

$$V_{2,4}^m = \langle V_{2,4}^m \rangle + V_{2,4}^m(t) \qquad (1.14)$$

In highly phase most of $V_2^{m,}{}_4$ is zero. In the distorted phase one (or more) of the coefficients Perfect Branch becomes zero and can be expanded in powers of order parameter Q =u

$$V = V_C + A_1 Q + A_2 Q^2 + . \qquad (1.15)$$

Taking into account the fluctuations of Q, above T_i

$$V = V_C + \sum_k A_1(k) Q(k) + \sum_k A_2(k_1, k_2) Q(k_1) Q(k_2) + \ldots \qquad (1.16)$$

For the EFG tensor tensor this expansion into more formal recording renaming symbols represented in the form [19,27]: at $T > T_i$

$$\langle V_{i,j} \rangle = V_{ij}^0(0) + A_{k2} \langle Q^c(k,t) \rangle + \ldots\ldots \qquad (1.17)$$

$$<\mathbf{V_{ij}}>=\mathbf{V_{ij}(0)}+S\mathbf{A_k}2<\mathbf{Q}^c\mathbf{(k,t)}>+... \qquad (1.17)$$

$$\left\langle V_{i,j}\right\rangle=\sum_k A_1(k)\delta Q(k,t)+\sum_{k1,k2} A_2^{/}\{\delta Q(k_1)\delta Q(k_2)-\left\langle \delta Q(k_1)\delta Q(k_2)\right\rangle\}+.....$$

$> T_i$ at $T> T_i$

$$\left\langle V_{i,j}\right\rangle = V_{ij}^0(0)+\sum_k A_1^{/}(k)\left\langle Q\ (k,t)\right\rangle+\sum_{k1} A_2^{/}\left\langle Q(k_1,t)\right\rangle^2+\sum_{k1} A_2\left\langle \delta Q(k_1)\delta Q(k_2)\right\rangle+.....$$

$$\left\langle V_{i,j}\right\rangle=\sum_k A_1(k)\delta Q(k,t)+\sum_{k1,k2} A_2^{/}\{\delta Q(k_1)\delta Q(k_2)-\left\langle \delta Q(k_1)\delta Q(k_2)\right\rangle\}+.....$$

where $\mathbf{Q(q_s-k,t)}$= áQ(q_s-k,t)ñ + d$\mathbf{Q(q_s-k,t)}$ - static and the fluctuation of the order parameter near the dew point of the soft mode q_s. The spectral function of a critical variable Q (k, t) has the form [19]:

$$G(k,\omega)=\int\left\langle V\ (k,0)V\ (k,t)\right\rangle\exp\{-i\omega t\}dt \qquad (1.18)$$

under decomposition and V_{ij} (k, t) may be represented as

$$G(k,\omega)=\int\left\langle|V^{/}(k,t)|^2\right\rangle v(k,t)\exp\{-i\omega t\}dt \qquad (1.19)$$

where V (k, O) V (k, t) is divided into static and temporal parts. If the time-dependent part of v (k, t) is a slowly varying function of time, for the wave vector q_s component of the spectral response function

$$\int G(q_S,\omega)d\omega=\left\langle|V\ (q_S,t)|^2\right\rangle : \left\langle|Q(q_S,t)|^2\right\rangle \quad (1.20)$$

with contributions by close to q_s, the line shape will be (taking into account the first term of the expansion)

$$\Gamma(\omega)=\sum_k\left\langle|Q(k,t)|^2\right\rangle g(k,\omega) \qquad (1.21)$$

thus the line shape reflects the shape of the distribution function of the atomic configuration of distortion caused by movement in slow-time radio. Linewidth characterizes while the rms value of the contributions to the distortion caused by the Fourier components of the displacement field with frequencies small compared to the reciprocal of the time threshold permits radio ($1/T^*_{Q.}$). If the low-temperature phase is observed any preferential swings from a position displaced by an amount ± Q_0(T)from the position of a highly, the line will consist of two components.

When T® T_i Q_0® 0 and splitting becomes small in comparison with (slow) fluctuations subtransient ordering. In the case of atom spectral line narrows to a minimum when the upper limit of the transition ordering. When a Q linear terms are comparable in

magnitude with quadratic, it is necessary to take into account the contribution of the relaxation processes in the Raman linewidth. Finally it should be noted that the lineshape Γ(w) is determined by all phonon wave vectors k . In view of this, it is necessary to analyze the results to have any model representation for g(k, w).

Expression (1.17) for the transformation of the EFG tensor near the phase transition indicates that studies of radiospectroscopic can extract information about the behavior of the order parameter Q (Qs-k, t).

Already at T> Ti measurements enable us to estimate <Q(t)> temporarily averaged square of the criticalcoordinates, which in the pre-transition region is associated with the critical dynamics. In particular, this refers to the crystals, where the phase transition is associated with an increase in the amplitude of the fluctuations caused by lattice vibrations or librational modes. Time-dependent part of the GEF determined by the speed and the type of processes with which the spin-lattice system can exchange energy.

Therefore, as follows from (1.17), can be studied microscopic dynamics of critical fluctuations amount of change in the fluctuations of the order parameter near $T_{i.}$

From the standpoint of radiospectroscopy question is how to properly excite the spin system and measure the spin-lattice relaxation time, to separate the various contributions and then link the measured values with the dynamics of critical fluctuations. In the case of nuclear NQR excitation system is an alternating magnetic field $H_{1.}$Hamiltonian describing the RF exposure to the system of nuclear spins in the case of continuous sensing has the form:

$$\overrightarrow{H_1} = 2\gamma hI\, H_1 \cos 2\pi\nu t \qquad (1.22)$$

where n - frequency of the RF field, g - gyromagnetic ratio.

The transition probability per unit time between the states c and c_1 in this case is given by [30,135]:

$$W_{kl} = \eta^{-2}\omega_{k1}Q(\nu) = \eta^{-2}|\langle\chi_k|I^*H_1|\chi_l\rangle|^2 G(\nu) \qquad (1.23)$$

W_{k1} –relative transition probabilities, G(n) - a function of the spectral distribution of the resonance line. Absorption intensity under resonant excitation depends on the difference in population levels and, in the absence of saturation, the expression [26,29]:

$$P_{kl} = \frac{N\nu^3}{\pi(2I+1)\Delta\nu kT} W_{kl} = \frac{n_0\eta\nu\gamma^2H_1^2T}{1+2\gamma^3H_1^3T_{Q1}T_{Q2}} = \eta\nu n_0\gamma^2 G(\nu)S \qquad (1.24)$$

N-number of nucleus , Dn - half-width of the absorption line.

Under pulsed excitation quantum spin system operators depend on time and to calculate the amplitude of transient signals commonly used density-matrix method [30]. In this case the change of the static density operator s is described by Neumann

$$\frac{d\mathsf{s}}{dt} = \frac{1}{\mathsf{h}}[\mathsf{s}, H]; H(t) = H_0(t) + H_1(t) + \qquad (1.25)$$

$\boldsymbol{H_0}(t)$ - the operator of the quadrupole interaction,

$\boldsymbol{H_1}(t)$ - operator interaction with the RF field H_1 cosnt. The last operator is zero between pulses. Equation is represented as [31,135] $\mathsf{s} = \mathbf{R}^{-1}\mathsf{s}_0\mathbf{R}$ where $\mathbf{R}=\mathbf{R_I}\mathbf{R_t}\mathbf{R_{II}}\mathbf{R_{t+t}}$. **$R_I$ and R_{II}**

solving the Schrodinger equation for the period action pulses (intervals nutation); $\mathbf{R}_t$ and $\mathbf{R}_{tt}$ -for free precession intervals between pulses

Developed methods for the solution of equation (1.25) allow us to calculate the amplitude of the signal induction $\mathbf{A}_t$, $\mathbf{A}_{t+t}$ and spin echo $\mathbf{A}_{t+t}$ with a two-pulse excitation of nucleus with spin 3/2 [32]. Spin echo envelope, as shown, may be represented by two terms - term proportional to the magnitude of the constant component and a corresponding member of the induction signal, which is small if $\mathbf{T}^*_{Q2} < t < \mathbf{T}_{Q2}$ ($\mathbf{T}_{Q2} \ll \mathbf{T}^*_{Q2}$). Study of spectral functions transient signals are not known. However, under certain spectral conditions, and in particular cases, referring to the direct comparison, it is reasonable to select those conditions of pulsed excitation, when the spectral shape of the resonant response is comparable to form a continuous sounding excited.

Referring to the description of known femenological model static and dynamic characteristics incommensurate phases [33,34].In the adiabatic approximation of the resonance line shape is described by the expression [27]

$$\Gamma(\nu)= \int_{-\infty}^{\infty} g(t)\exp(-i\nu t)dt \qquad (1.26)$$

where $g(t) = \left\langle \exp\{ \int_0^t \eta(t')\,dt' \} \right\rangle$

that looks like a static redistribution

$$G(\eta) = \int_{-\infty}^{\infty} \langle V(t)\,V(0)\rangle \exp(i\eta\, t)\,dt = \int g(\eta - \eta_C)\,A(\eta_C)\,d\eta_C \qquad (1.27)$$

If we assume that at the phase transition, the frequency of the resonance absorption of the nucleus can be expanded in powers of the displacements

$$\eta_i = \eta_{0i} + A_{ij}u_i + A_{2i}u_i^2 + A_{3i}u_i^3 + \ldots\ldots \qquad (1.28)$$

where u_i can be represented as an expansion in the eigenvectors of the soft mode (1.1), for each atom **p** varieties can write (nonlocal description) [35]:

$$u_{ip} = u^C_{0p}\cos((x_i)) + u^S_{op}\sin((x_i)) \qquad (1.29)$$

where the plane-wave approximation modulation (PWA), the phase changes of the atomic displacements *as:*

$$\mathbf{j\ (x)\ = q_s x_p + j\ _{op}(x);} \qquad (1.30)$$

and in the soliton approximation:

$$\varphi(x)=\varphi_{op} + \frac{2\pi m}{p} + \frac{m}{p}\,\mathrm{arctg}\{\exp(-\alpha(x-mb)\sqrt{p})\} \qquad (1.31)$$

If the modulation long periodic then

$$q_S = (1-\delta)a^*/p = q_C - \frac{N}{M}q_C$$

After substituting (29) into (28) we obtain

$$\nu(X)=\nu_0+\nu_1\cos(\psi(x)+\varphi)+\nu_2^{/}+\nu_2\cos^2\psi(x)+\ldots \qquad (1.32)$$

The density of the spectral function **f(n)** according to [33] will be determined by the expression:

$$f(\nu)=\frac{N}{|\P n/\P j\ |}=\frac{N}{(\P n/\P j\ )(\P y\ /\P x)} \qquad (1.33)$$

where are N - the number of nucleus per unit length in the direction of the incommensurate modulation. In the case of long-period of modulation **f(n)** represents the sum of the discrete frequency components of each unit cell unit .

The specific form of the expansion is determined by the local crystal symmetry and lattice site for which the expansion is made, namely, the symmetry of the electronic environment and the symmetry of the eigenvectors of the soft mode. This imposes restrictions on the type of decomposition (1.28), and some of the coefficients $\mathbf{A_{ki}}$ may be zero ($\mathbf{A_1}0$, $\mathbf{A_2}=0$ - linear expansion, $\mathbf{A_1}=0$, $\mathbf{A_2}0$ - quadratic expansion, etc.).

Analysis of the function **f(n)** was carried out for all sorts of occasions decomposition n(x). First results were obtained under the assumption that the resonance frequency $\mathbf{n_{o1}}$ working nucleus depends only on the in-phase shifting him atoms (local description) [34]. For illustration, Figure 1.3 shows a view of functions **f(n)** and thermal splitting of boundary singularities on the situation for high-symmetry phase in the case of a quadratic approximation PVM.

Later, it was considered femenologicheski impact on GEO Dunn nucleus atomic displacements of the nearby environment associated with other eigenvectors of the soft mode (nonlocal description) [35]. In this case it was possible to achieve greater agreement with experiment. From a theoretical point of view and questions analyzed the spin-lattice relaxation of nucleus in incommensurate systems [33,35].

Thus there is a theoretical basis for the description of the resonance spectra in neoorazmerennyh systems, both static and dynamic aspects. Experimental research objective is to obtain data for comparison.

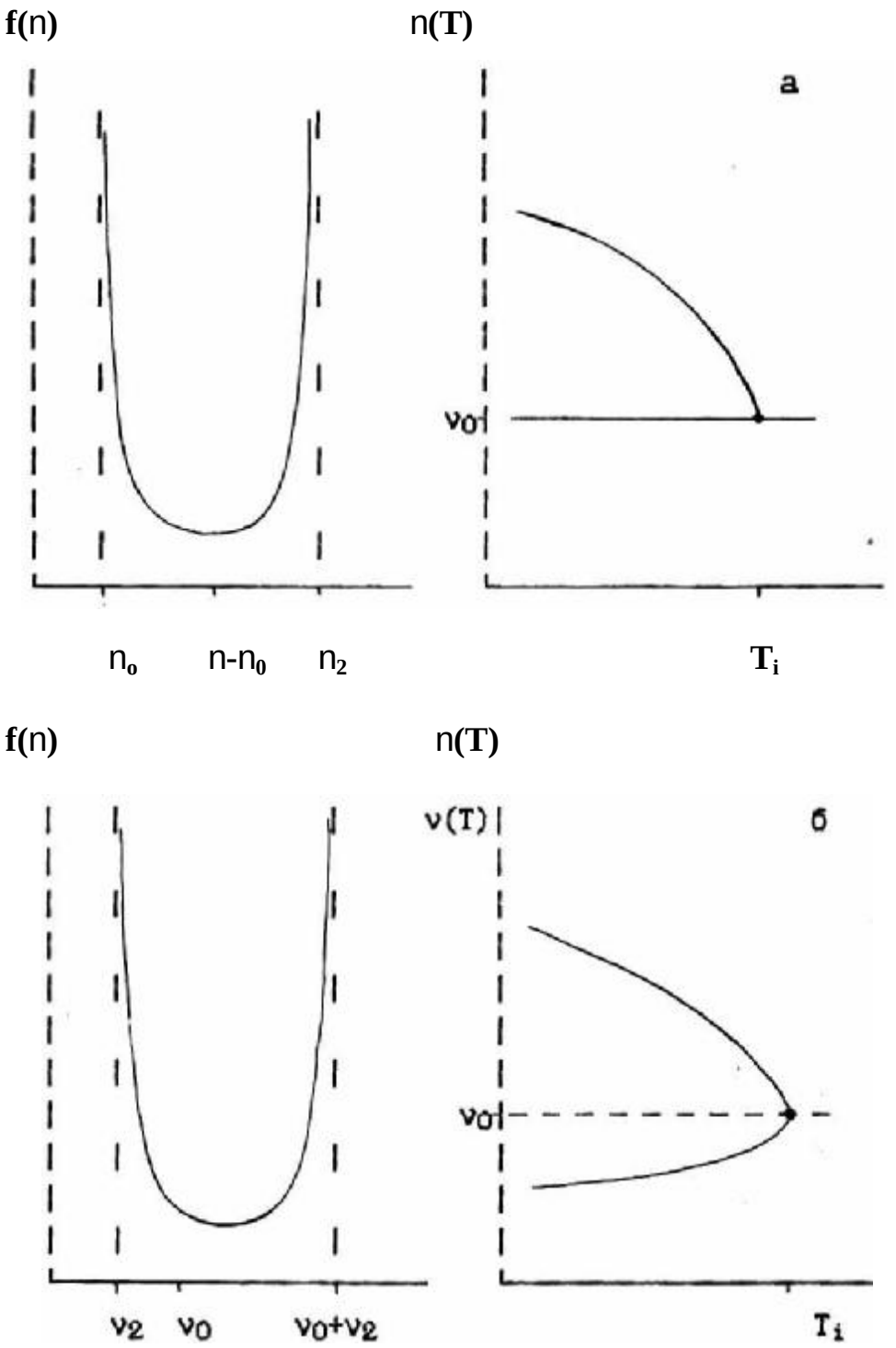

Figure 1.3. Type function **f(n)** and when disconnection of frequencies in T_i a) local and b) nonlocal cases.

§ 1.3 Experimental studies of families of compounds A_2BX_4 structure type β-K_2S0_4.

By now, several hundred compounds of the chemical composition A_2BX_4 (A = K, Na, Rb, Cs, NH_4 ...; B = Zn, S, Co, Mn, Cd, Mg, Se; X = F, Cl, Br, J. ..) with an octahedral, tetrahedral, and planar coordinations distorted anion X, relative to the atoms of type A 170 from various structures such composition is one of the most interesting type structure β-K_2SO_4, wherein the coordinating anion is close to the tetrahedral . In recent years, representatives of this structural type attract attention due to the discovery disproportionately modulated phases in compounds β-K_2SO_4 [2], Rb_2ZnCl_4 [39], K_2ZnCl_4 [37], Rb_2ZnBr_4 [38], $(NH_4)_2ZnCl_4$ [39], Cs_2HgBr_4 [46] and others.

High-temperature phase β-K_2SO_4 is orthorhombic and space group D_{2h}^{16}(Pnma) (b>a>c) [40]. It is also assumed that this structure is praphase nonpolar structure with space group symmetry $D_{6h}^{4}(P6_3/mm_6)$. This structure was observed above T = 745K in K_2SeO_4 [58].

On the basis of structural studies in the literature formed the view that the diversity of family structures in the A_2SBHal_4, due to the high porosity of the core nucleus halogens and volatile cations A relatively small perturbation of the electron configuration of anions The connection A-A' in some cases resembled relation H-H'with two minimumnym potential [128].

Crystal-structure analysis of stability β-K_2SO_4 [4] made based on a comparison of anionic and cationic radii in the problem of dense packing gives the forecast for the region of stability of the structure (Figure 1.4). Experimental data indicate that the most structurally diverse compounds properties are located on the border of stability of structure β-K_2SO_4. Such compounds with various external effects exhibit, as a rule, a tendency to a sequence of phase transitions in less symmetrical, manner in the structural hierarchy, phase. In this sequence and implemented disproportionately modulated structure. In addition, the analysis of the crystal-chemical and experimental data indicates the possibility of the existence of another type of instability ion frame associated with symmetry-unrelated transformation structure.

Modulated phases owe their existence delicate balance intracrystalline interactions, which, as experience shows, can be easily broken. Preliminary theoretical studies of these interactions indicate that itself modulated structure can be represented by a sequence of higher level of symmetry. On the basis of these results, the physics can expect the discovery of new principles describe the crystalline state and the detection of previously unknown properties of dielectric solids.

Currently, research efforts are focused on the one hand to find and codify different structures in the incommensurate phase and a generalized phase diagram of these compounds and, on the other hand, figuring out the new features and capabilities to manage these structures.

Until the moment of this writing the most studied compounds were presented in Table 4.4. They all have high-temperature phase with the space group symmetry D_{2h}^{16} (Rnma) and with decreasing temperature test sequence of phase transitions. Presented in Table compounds can be divided into three groups according to the position of the symmetry in the Brillouin cell dew point of the soft mode: near the S-line, L-line and **X**-line.

Incommensurate phases observed in these compounds have one-dimensional modulation, characterized by displacement of the atoms along the **a, b** or **c** directions "direct" lattice. As the temperature decreases observed sequence of phase transitions between phases with space group symmetry, which are sufficiently consistent scheme developed in [18]. The experimental data presented in the table 4.1 were obtained with the assistance of various macroscopic and structural measurements. All of these compounds were investigated radiospectroscopic methods. In most of the compounds detected the presence of

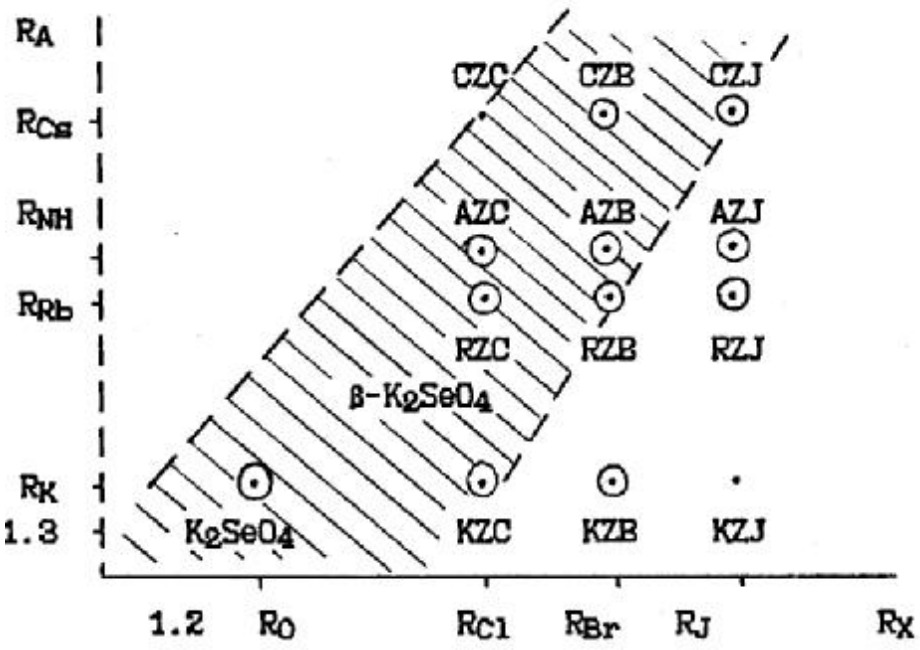

Figure 1.4. Stability domain structure β-K_2SO_4 for compounds A_2ZnX_4. (See the notation in Table. 3.1)

an incommensurate phase NQR, NMR and EPR. Below we will focus mainly on the NQR studies, and the results of other resonance techniques will attract only as needed As seen from Table 4.1, most of the nucleus of atoms of compounds have a nonzero quadrupole moment. However, from a practical point of view, are the most suitable halogen isotopes: J, Br and Cl. The nucleus of the lasttwo have spin 3/2, and according to theory NQR can be in two doubly degenerate energy states [43]:

$$E_{1,2} = \frac{e Q q_{zz}}{4} \rho ; \rho = \left(1 + \frac{\eta^2}{3}\right)^{1/2} \qquad (1.33)$$

where Q - quadrupole moment; h - the asymmetry parameter; q_{zz} - EFG component along the main axes of the tensor $q_{ab.}$ In the absence of disturbances, for there is one observation of the NQR frequency

$$\nu_{1/2-3/2} = \frac{1}{2} e Q q_{zz} \rho , \qquad (1.34)$$

change that is required to change the EFG at work at the core of the structural phase transformations. On the measurement of the NQR frequencies of non-equivalent structural positions of the nucleus based simplest methods NQR.

For quantum transitions between levels of quadrupole nucleus with spin different from 3/2 with more than two non-degenerate transitions, which is possible to observe the effect of "pure" NQR [24]. The most common methods of NQR are stationary when the spin system affects continuous RF field and unsteady - recorded when the system response to impulse action.

First NQR data in compounds A_2BX_4 (X-halogen) have been presented in [44,45]. For a large group of compounds bysuper-regenerative spectrometer were measured NQR frequencies at room temperature and the boiling point of nitrogen. It was noted that in some compounds the signals are not observed or observed only partially and incontradiction with the diffraction structural data The pioneering research NQR incommensurate phases were performed in in IF SB AN USSR A.K.Moskalev and et al. [36] and IN&OCh AS USSR G.K.Semin [46]. In these papers to study incommensurate phases was applied pulse NQR method. In the first of the cited work was to study the evolution of the NQR spectra in the crystal Cs_2ZnCl_4 and built the temperature dependence of the frequency dependences of nucleus $^{35}C1$ (Figure 1.5). [46] studied the compounds Cs_2HgBr_4, where the authors observed NQR spectra in the incommensurate phase. Following work was performed at the junction of Rb_2ZnBr_4 [38], where the NQR spectra were studied in the incommensurate phase and frequency dependence is built in a wide temperature range (Figure.1.5b).

Given the experimental data of [36,33,38] on the basis that existed at that time, theoretical ideas about the disproportionate state model was proposed femenologicheskaya cancellation resonance line shape evolution in the incommensurate phase [33]. The frequency distribution of NQR spectra have been analyzed in the framework of the plane-wave approximation and the soliton. On the basis of the calculated line shape fit to the experimental qualitative agreement was reached with the description of the proposed model of the incommensurate phase in the framework of the plane wave approximation [34]. However near T_C agreement was unsatisfactoryIn this area, there was an attempt to describe the theory of Dzyaloshinskii-Landau, through the concept of identifying the

density of solitons with the order parameter of the phase transition to the ferroelectric phase.

Another attempt to study the incommensurate phase was undertaken in K_2ZnCl_4 stationary NQR method [37]. At room temperature, as in [44], with the resonance lines 6 ^{35}C1. However, in the incommensurate phase NQR signals were observed only near $T_{i,}$ the position (I) C1^{35} nucleus in the structure Pnma. The absence of signals from other nucleus ^{35}C1 explained significant reorientation of the $ZnCl_4$ tetrahedra around its axis passing through the position of the nucleus Cl(1) and coincides with the axis symmetry structure.

In 1980 he was made a comprehensive study of the compounds Cs_2HgBr_4 and Cs_2CdBr_4 [48] and the observed sequence of phase transitions shown in Table 4.1. Using pulse technology NQR was tracked the temperature dependence of the frequency, while in the incommensurate phase NQR signals were observed only on the position. I core structure Rnma ^{81}Br. Line shape in the Jc-phase had continual distribution and attempted to describe it as part of the plane wave approximation model [33].However pronounced asymmetry form was not explained clearly. Signs soliton picture offset was observed.

Compound $(NH_{4)2}ZnCl_4$ and $(NH_{4)2}ZnJ_4$ also were first investigated by NQR in Krasnoyarsk **IF** [39,49]. In the first of these compounds, in the temperature range from 271K to 266K, anomalous behavior of NQR spectra in which 16 high-temperature phase of singlet lines are mapped to 12 NQR lines below 266K. In the intermediate temperature range was registered incommensurate phase. In $(NH_{4)2}ZnJ_4$ similar type anomaly was observed at 222K in 4K (Figure 1.6). In these compounds, involving other methods, later was detected and other phase transitions indicated in Table 4.1.

RF methods have been reported and studied incommensurate phases in the $(NH_{4)2}BeF_4$ and $\{TMA\}_2ZnCl_4$ (see the references in [33]).

Thus, a simple observation made by NQR can detect incommensurate phases.

Simultaneously with the work described above, for several years compounds with β-K_2SO_4 and studied all sorts of other methods, and to date there is sufficient information on the properties of the phases and characteristics of phase transitions for each compound. The major method allows to measure directly the value of q_s are diffraction methods.

The main advantages of pulsed rf is the possibility of direct measurement of the spin-spin T_{q2} and spin-lattice relaxation time T_{q1} system. This information, as noted above, is of great value for the study of the dynamics of the system in a critical phase transition region.

Blintz and coworkers [33] were measured by NMR $T_{Q1}(T)$ and $T_{Q1}(n)$for the core ^{87}Rb in the compounds Rb_2ZnBr_4 and $Rb_2ZnClBr_.$ Results were compared with theory. In the P-Jc transition usually observed critical shortening $T_{q1,}$ which, as stated by the authors, was not contrary softly-mode description. In Jc phase in a wide temperature range T_{q1} ivmenyaetsya little with temperature and is abnormally short. Originally it was explained the predominant influence of phason excitations in the entire region of the incommensurate phase. However, studies in the high part of the measurement phase and Jo T_{q1} in metered-doped solid solution $(Rb_{1-x}K_{x)2}ZnCl_4$ (x = 0, 0.02, 0.06) [52] reported significant influence of impurities on the behavior of T_{q1} in Jc phase transition at T_C At x = 0, the value T_{q1} was reduced and observed at T_C T_{q1} races.

In conclusion, the experimental part of the review, we note some kinetic phenomena observed in the incommensurate phases. In studies of systems with dipole density waves

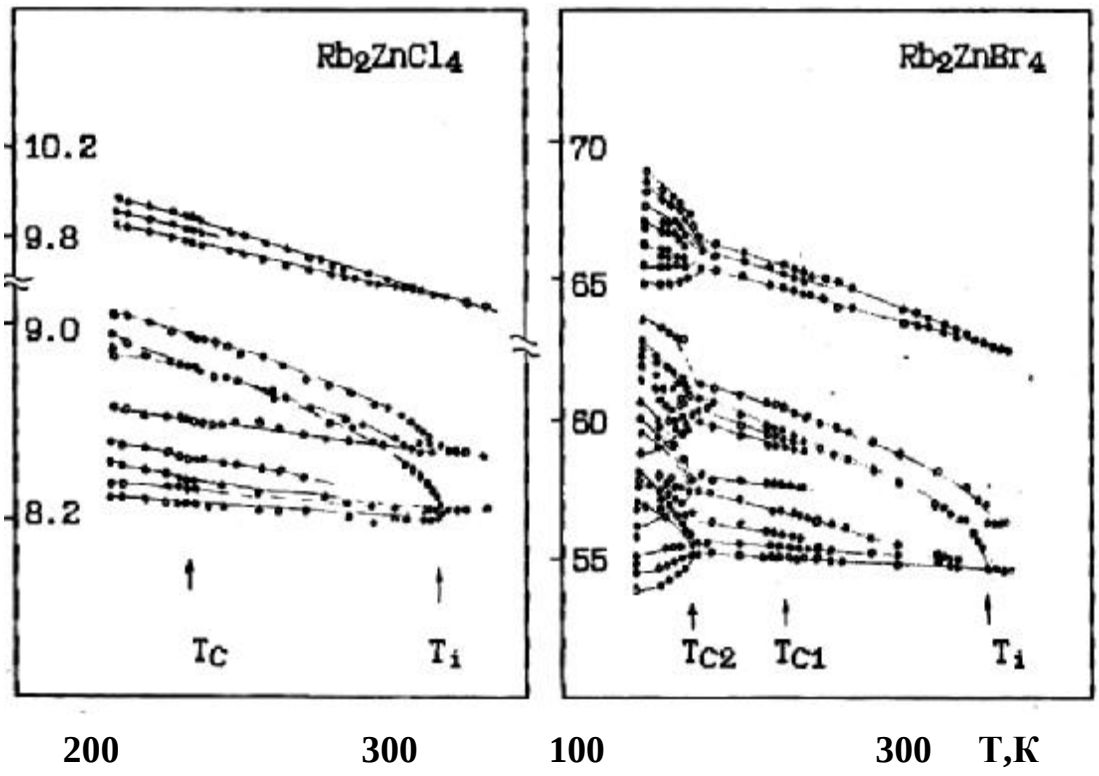

Figure 1.5. Temperature dependence of the frequency of the NQR lines of Rb_2ZnCl_4 and Rb_2ZnBr_4

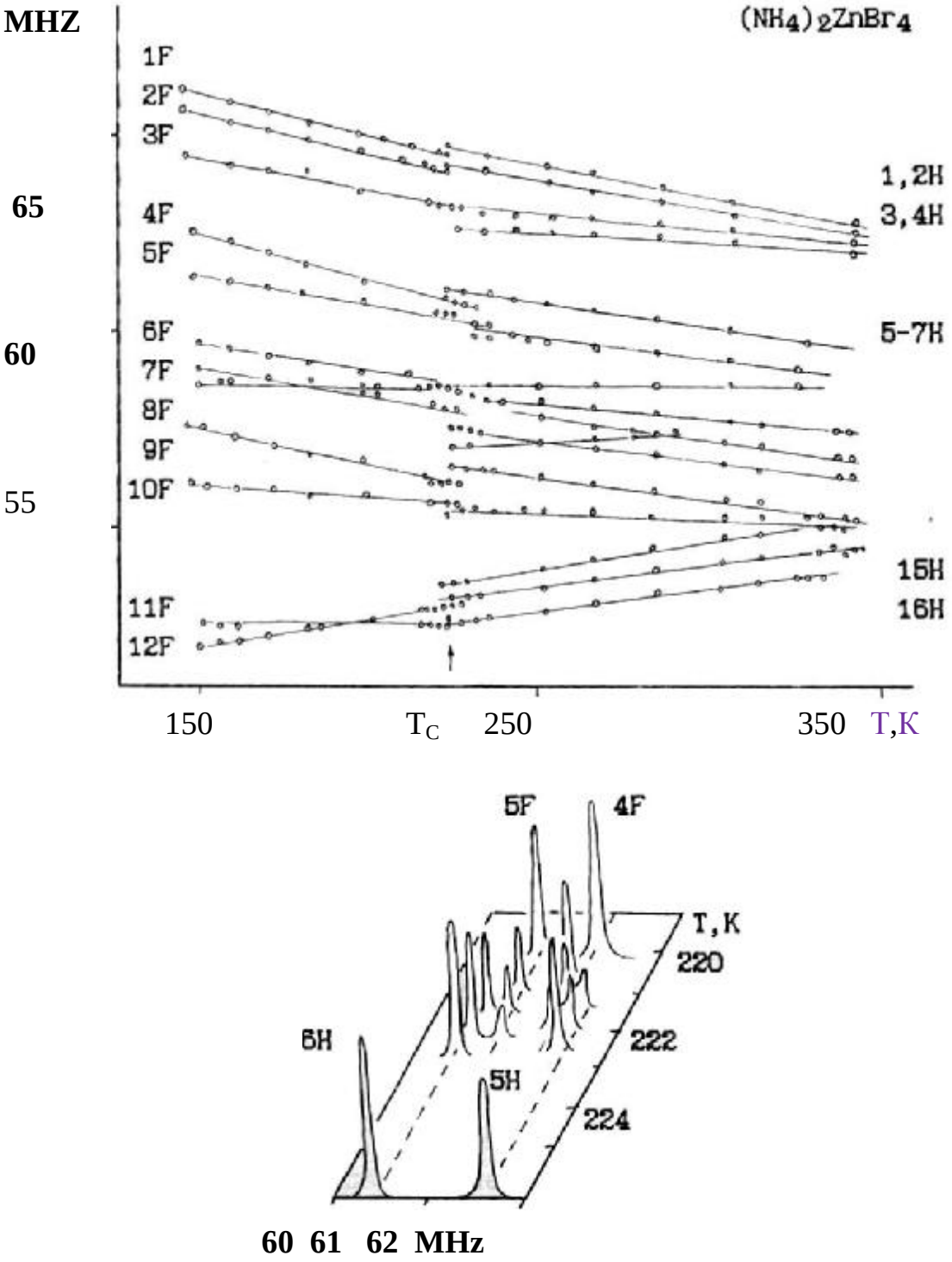

Figure 1.6. Temperature dependence of the frequency and the change in T_C line intensity 5F and 6F NQR spectrum in the $(NH_4)_2ZnBr_4$.

(which include dielectrics and modulated with a structure of β-K_2SO_4) in the incommensurate phase were found by macroscopic nonequilibrium processes that are a little earlier, were seen in systems with charge density waves [63]. One of these phenomena, called global hysteresis is the presence of a kind of hysteretic behavior was observed in the entire region of the incommensurate phase [60,62]. A typical illustration of this behavior is mutually reciprocal transition between states I« II characterized by the magnitude of the inverse susceptibility 1/(c-c_o) (corresponding to the cooling mode (I) or heating (II) when the direction of the sample temperature in the opposite Jc phase near T_C [62]). When the temperature stop $T_{stop} > T_C$ trend approximation value 1/(c-c_o) to some equilibrium state III. However, if after stopping, the direction of change of temperature is stored, the temperature during the reverse stroke, when the temperature T'_S observed small leap 0.01% of the measured macroscopic susceptibility. The temperature T'_S, up to a temperature hysteresis stop coincides with the temperature T_S [61]. This phenomenon has been referred to the effect of thermal memory. Additionally in studying samples doped Rb_2ZnBr_4, it was found that the form of the hysteresis curves of dielectric measurements depends on the prehistory of the sample [60]. Initially, these nonequilibrium phenomena explained by the interaction of the modulation wave soliton configurations with mobile defects. In this model competition soliton-soliton and soliton-defect interaction at fixed external conditions for quite a long time leads to the establishment of a quasi equilibrium system micro configuration. Conditions change and subsequent recovery, after a time shorter than the diffusion of defects, their distribution is correlated with the quasi-equilibrium conditions for the data configuration of solitons. However, theoretical estimates to quantify the magnitude of this effect in real crystals [62], as well as direct electron microscopic observation of the actual configuration of the walls transform domain disproportionate Rb_2ZnCl_4 and 2H-Ta_2Se [53] pointed out that the main mechanism of the transformation of the soliton strktury are the processes of formation (destruction) of anti-germ incommensurate phase (stripple nuciies) [62,63]. The unit consists of a single nucleus (P = 2) or more (P > 2) regions with incommensurate structure, surrounded on all sides by the other incommensurate structure. Structures differ in the magnitude of the phase

$$j_{li} = j_O \frac{2\pi}{p} n_{li}\ ; \quad (n_{li} = -(p-1),\ -1,0,+1..\ p-1))$$

and separated soliton walls. The walls of the embryo in their intersection to form a special (topological) defect. With the growth or dissolution of embryos there are significant elastic force impeding change its volume (in the case of the strong interaction of the topological defect with a matrix structure of the crystal). Due to this, the system has significant internal friction, preventing movement of the defect and an inhomogeneous stress. Development of the latter may result in an increase of the same type at the expense of other domains, as well as affect the amount of phase change in the domain walls

$$j - \frac{2\pi}{p} j_O \ ^1 \quad 0$$

§ 1.4. Investigation of incommensurate phases in dielectric crystals at high pressure.

After the initial accumulation of experimental information. Study of incommensurate phases in the temperature scale, its amount was insufficient to prove or disprove any of the theories disproportionate state. Efforts experiments were aimed at expanding research using other external parameters. One of them is thehydrostatic pressure

Fig. 1.7 and 1.8 shows the phase P-T diagram of some compounds. These diagrams have been prepared by various methods. The most important from the point of view of the structure are the diffraction data. One of the first studies of molecular dielectrics with an incommensurate phase at high pressure was performed on a crystal of thiourea $SC(NH_{4)2}$ Fig.1.7 [53]. In this connection method neutron diffraction were tracked change in pressure of the wave vector of the incommensurate modulation. At atmospheric pressure, J_C phase due to softening of one of the static modes in the center of the Brillouin zone. Under pressure dew point is marked deviation from the center of fashion, followed by a tripling of the unit cell volume.

In $NaNO_2$ incommensurate phase is also associated with the softening of one of the modes of nature relaxation at zero frequency. In this connection disappears incommensurate phase at low pressures, is also assumed that the incommensurate phase in Cs_2HgBr_4 disappears when the load [54].

Any studies under pressure this class of compounds by RF unknown to us. Among the compounds having ferroelectric properties and having, as it turned out during our research, incommensurate phase, work on the high pressure NQR was held on proustite Ag_2 AsS_3 Fig.1.76 [56,57]. It has been suggested disappearance incommensurate pressurized state. P-T phase diagrams of some of the compounds A_2BX_4 were initially identified using dielectric measurements. Figure. data obtained are presented in [58], and Fig.1.8b in [59]. The first type of compounds with a structure β-K_2SO_4 studied in detail the crystal was pressurized $\{TMA\}_2ZnCl_4$ (Fig.1.7b) [55]. Neytron diffraction method it was filmed isothermal variation of the wave vector $q_{S,}$ traced the region of existence of the incommensurate phase and found a structure with multiple larger unit cell. Character changes q_S adequate behavior such as "devil's staircase". Thus by the time of our study were quite scarce data on disproportionate phases under pressure, and most of them have been published during the execution of our program.

From the analysis of the physics of incommensurate systems in dielectrics family A_2BX_4 structure β-$K_2SO_{4,}$ it is seen that there is a broad range of issues requiring further experimental clarification. First, the lack of detailed structural data on family type β-$K_2SO_{4,}$ where at the beginning of our work was carried out initial studies of all seven of its representatives (of 25 projected).

The resulting macroscopic diffraction and radio spectroscopy data indicate significant differences in the structural transformation of compounds as the wave vector and sequence of structural transformations. In various compounds below the transition to the incommensurate phase was observed significantly different multiplicity spectra and different degree of ordering of the structure dynamics. Not quite clear was the question of

uniformity of phase transitions P « J_C and J_C « F. Also highlights some of the difficulties in explaining the shape of the line in the incommensurate phase on the basis of

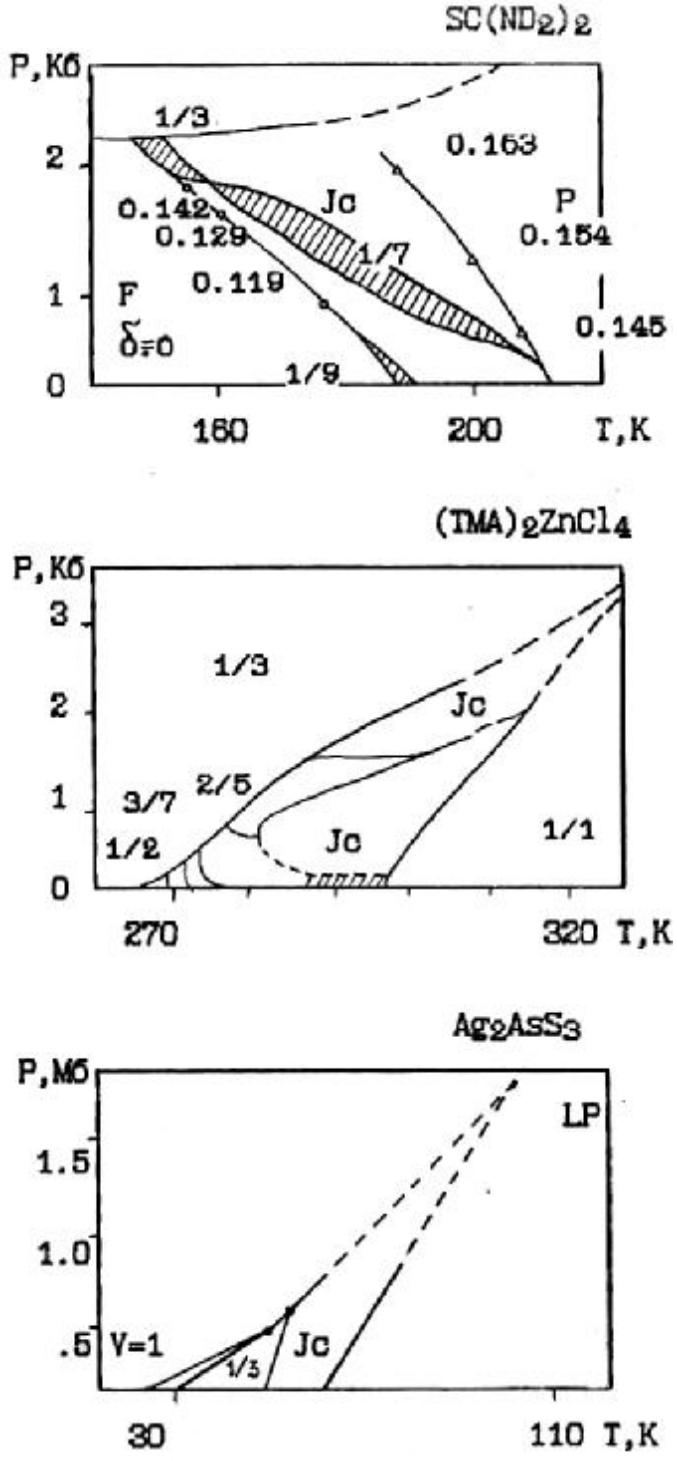

Figure 1.7. Phase diagrams of dielectrics: a) thiourea; b) $(TMA)_2ZnCl_4$; c) proustite.

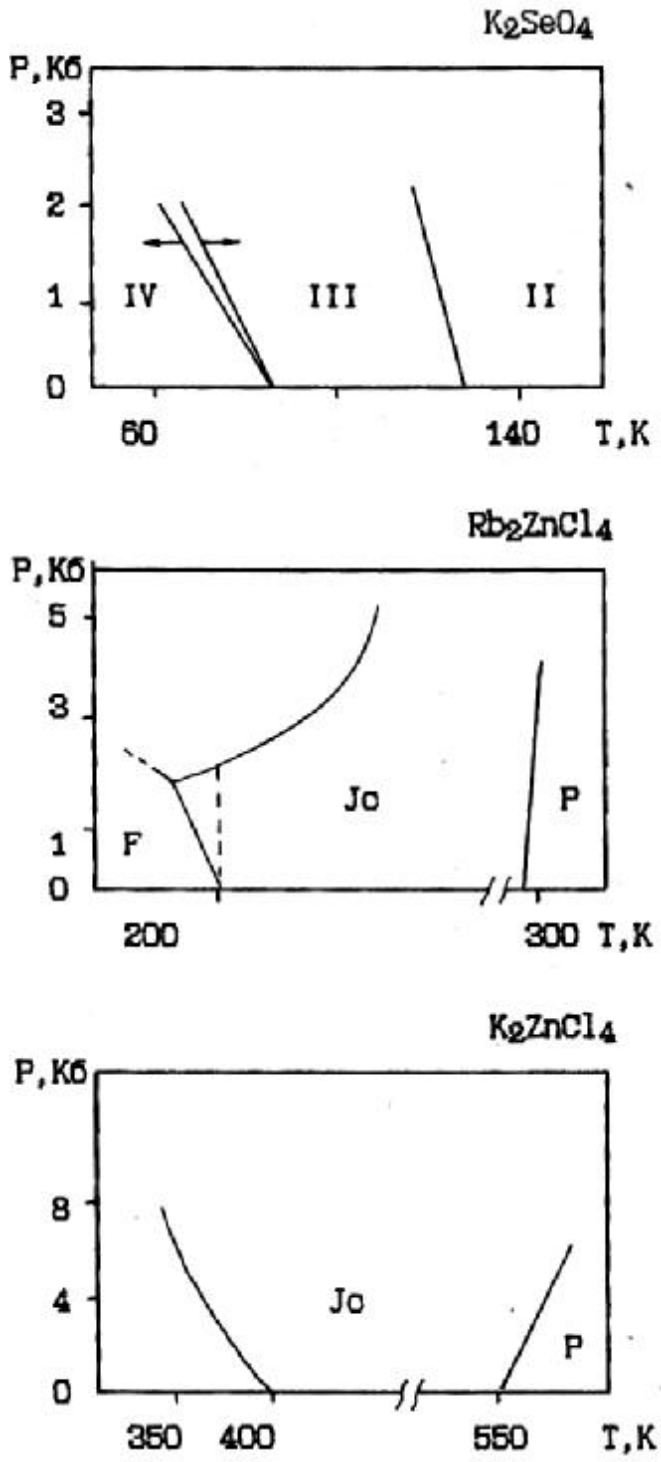

Figure 1.8. P-T phase diagrams of compounds A_2BX_4 obtained by -measurements.

continuous semiclassical theory Dzyaloshinsky-Landau, whereas non-classical type theory Izinga indicate the behavior of complex or simple type "devil's staircase".

Because NQR method, in many cases allows a quantitative interpretation of the structural and dynamic transformations near phase transitions, as well as to feel a slight change in the local structural environment of the quadrupole probe subsystem of the crystal, there is a strong, virtually confirmed the reasons for its use in the study of the subject systems. Even the simplest information to monitor changes in multiplicity intensity and width NQR lines contains important information about changes in the crystal structure and chemical environment, the nature of phase transitions and spin dynamics. More detailed studies, such as the study of the frequency dependences of ν (T), I (T), uv (T) and the change of the relaxation times T_Q T_{Q1} and $T_{Q2,}$ and others, allows to draw conclusions about the type and nature of the motion of molecular segments or electronic excitations directions of chemical bonds, etc. The advantage of NMR NQR before the winner is sensitivity at high frequencies >10 MHz, where exactly are the NQR frequency halogen nucleus belonging to the majority of the members of the family A_2BX_4. Furthermore NQR has the advantage of relative simplicity of the experimental formulation, especially at high hydrostatic pressure. This simplification, however, made up for the back while trying to implement a tribute to the experimental data in the options atomic motions as a microscopic theory of the quadrupole relaxation is based on the specific solid model and crystal chemical bond theory, which, as you know, in these compounds, only beginning to be developed. NQR advantage before EPR - not violated local electronic environment of the matrix.

Tetrahedral or close to the structure of segments BX_4 not densely packed β-K_2SO_4, leads us to expect the possibility of significant local and collective distortion when the external parameters. And it can be assumed that with the NQR method should be obtained valuable, in terms of solid state physics and phase transitions, information. Experimental task in the first stage is a generalized phase diagram β-K_2SO_4. On the other hand one can study the structure of the electronic environment of the nucleus - a task more difficult and laborious, and most successfully solved in the presence of all primary data from NQR, NMR and diffraction methods for all compounds of group A_2BX_4 structure β-K_2SO_4.

We have formulated the following research areas:

1) Controlled diffraction and NQR synthesis of compounds A_2BX_4 major cations and anions (A = NH_4, Cs; B = J), near the border the crystal structure stability β-K_2SO_4, to detect them with this structure sequence of phase transitions involving incommensurate phase.

2) Application of the method of NQR under high pressure to determine the domains of existence of the structural evolution of J_O phase in Rb_2ZnBr_4 under high hydrostatic pressure. A more detailed study of the NQR (in combination with other methods) Rb_2ZnBr_4, to find in this connection behavior such as "devil's staircase" or long-period structures.

3) Explanation of the reasons for the unsatisfactory description of the forms of radio frequency absorption lines in the incommensurate phase of Rb_2ZnBr_4.

In preliminary studies, after setting growth compounds A_2BX_4 with major ions and detection in a number of these structures β-K_2SO_4, scheduled tasks were also associated with an additional question:

4) Assessment of the degree of spin-phonon, spin-spin dynamics in the synthesized compounds.

Chapter 2. Equipment and measurement technique.

§ 2.1. Receiver sensitivity sensor NQR and conditions optimum adaptation to the measuring chamber.

As is known, the sensitivity of the receiving path to radio spectrometer NQR absorption signals defined set of parameters [27]. Thus, according to the survey [64], S / N ratio of the signal to noise ratio at the receiver output can be represented as:

$$S/N= \frac{\alpha N Q \xi r^2}{\sqrt{4kB)QN^2\nu_0 T_r \sqrt{r+R_{ecv}T_{ecv}}}} \qquad (2.1)$$

where a - nuclear spin contribution, N and r - the number of turns and the radius of the solenoid, Q - Q-factor of the receiver coil, B - receiver bandwidth, T_c - temperature of the resonator, ξ - the filling factor of the resonator, R_{eq} T_{eq} - equivalent resistance and temperature receiver, ν_o - quadrupole resonance frequency.

In this section we will carry out examination of the conditions that must be considered when designing NQR cameras to increase the quality factor of the receiving circuit. As is known, this value is limited by the condition $Q < 1{,}5\nu_o\tau_{im}$ where τ_{im} - lifetime free induction signal. In NQR typically Q <150. However, the location of the sensor in the NQR shell, which is a body of a device external influence on the sample, the Q value is significantly reduced due impendansnoy sensor communication with the shell of the device. This relationship can be expressed as follows [65]:

$$Q=\frac{\nu W}{P} \qquad (2.2)$$

where W - energy stored in the resonator, P-power loss associated in particular with the dissipation of energy in the environment of the resonator. To calculate the losses it is necessary to estimate the energy W. As we know the energy of interaction between two conductors is expressed through the inductive factor $\mathbf{L_{12}}$

$$W_p=\frac{1}{8\pi}\int_V \vec{H}\vec{B}\,dV \;:\; \frac{L_{12}J_1J_2}{C^2} \qquad (2.3)$$

where J - volume currents. In case the interaction of the solenoid (radius **r** and length **l(1)**) with a cylindrical shell (radius **R**, the length **L** and the thickness **H**) according to [66] has an analytical expression:

$$L_{1/2}=\sum_{k-1}^{N}\int_0\int_{-1/2}\frac{r(R+H/2)\cos\varphi\,d\varphi\,dL}{\sqrt{\left(\frac{L-1+1/N}{2}-k\frac{1}{N}\right)^2+\left(R+\frac{H}{2}\right)^2+r^2+2\left(R+\frac{H}{2}\right)r\cos\varphi}} \qquad (2.4)$$